Pentapeptide-repeat, cytoplasmic-membrane protein HglK influences the septal junctions in the heterocystous cyanobacterium *Anabaena*

Sergio Arévalo and Enrique Flores*

Instituto de Bioquímica Vegetal y Fotosíntesis, Consejo Superior de Investigaciones Científicas and Universidad de Sevilla, Américo Vespucio 49, E-41092 Seville, Spain.

*For correspondence. Tel.: +34954489523; E-mail: eflores@ibvf.csic.es.

Running title: HglK influences septal junctions in *Anabaena*

Key words: Bacterial development; Cyanobacteria; Heterocyst differentiation; Intercellular communication; Nitrogen fixation; Pentapeptide-repeat protein; Septal junctions.

Summary

N_2-fixing, heterocystous cyanobacteria grow as chains of cells that are connected by proteinaceous septal junctions, which traverse the septal peptidoglycan through nanopores and mediate intercellular molecular transfer. In the model organism *Anabaena* sp. strain PCC 7120, proteins SepJ, FraC and FraD, which are localized at the cell poles in the intercellular septa, are needed to produce the septal junctions. The pentapeptide-repeat, membrane-spanning protein HglK has been described to be involved in the deposition of the heterocyst glycolipid layer, but the *hglK* mutant also showed intercellular septa broader than in the wild type. Here we found that an *hglK* mutant of *Anabaena* is impaired in the expression of heterocyst-related genes *coxB2A2C2* (cytochrome *c* oxidase) and *nifHDK* (nitrogenase), indicating a defect in heterocyst differentiation. HglK was predominantly localized at the intercellular septa and was required to make long filaments, produce a normal number of nanopores, and express full intercellular molecular transfer activity. However, the effects of *hglK* inactivation were not additive to those of inactivation of *sepJ* and/or *fraC-fraD*. We suggest that HglK contributes to the architecture of the intercellular septa with an impact on the function of septal junctions.

Introduction

Heterocystous cyanobacteria grow as chains of cells that, under deprivation of combined nitrogen, contain two cell types: vegetative cells that fix CO_2 through oxygenic photosynthesis and heterocysts specialized for the fixation of atmospheric nitrogen (N_2) (Herrero *et al.*, 2016). Heterocysts are formed by differentiation of vegetative cells, and in cyanobacteria of the order Nostocales heterocysts are frequently found with a spaced pattern of about one heterocyst per 10 to 15 vegetative cells (Wolk, 1996). The differentiation of a vegetative cell into a heterocyst results from a distinct program of gene expression, which involves the successive expression of regulatory and structural genes, the latter encoding proteins that produce the morphological changes inherent to heterocyst formation and the enzymes that execute heterocyst metabolism (Flores *et al.*, 2018). The most evident morphological changes include (i) the deposition of an extra cell envelope, which is composed of heterocyst-specific polysaccharides (Hep) and heterocyst-specific glycolipids (Hgl); (ii) the rearrangement of intracellular membranes, which are re-localized next to the cell poles and change from performing oxygenic photosynthesis to anoxygenic photosynthesis and respiration; and (iii) the development of distinct cell poles where the cytoplasmic membrane and cytoplasm are constricted and a cyanophycin (multi-L-arginyl poly [L-aspartic acid]) plug is deposited (Flores *et al.*, 2018). These morphological changes, together with the expression of O_2-consuming enzymes (Valladares *et al.*, 2003; Ermakova *et al.*, 2014), make the heterocyst appropriate for *nif* gene expression and nitrogenase function (Elhai and Wolk, 1990; Pratte and Thiel, 2016).

Intercellular transfer of regulators of heterocyst differentiation and nutrients takes place in the cyanobacterial filament (Herrero *et al.*, 2016). Cyanobacteria are diderm bacteria (i.e., they bear a Gram-negative type of cell envelope), and in filamentous cyanobacteria each cell is surrounded by its cytoplasmic membrane and peptidoglycan layer(s), whereas the outer membrane is continuous along the filament (reviewed in Hahn and Schleiff, 2014). Cells in the filament are joined by septal junctions (Flores *et al.*, 2019), which traverse the septal peptidoglycan layers through nanopores that are visible by transmission electron microscopy of

whole filaments (Wilk *et al.*, 2011) or of isolated murein sacculi (Lehner *et al.*, 2013). Fluorescent markers –calcein, 5-carboxyfluorescein (5-CF), and the sucrose analogue esculin– have been used to probe intercellular molecular exchange in filamentous cyanobacteria (Mullineaux *et al.*, 2008; Mariscal *et al.*, 2011; Nürnberg *et al.*, 2015). In the model heterocystous cyanobacterium *Anabaena* sp. strain PCC 7120 (hereafter *Anabaena*), proteins localized at the intercellular septa that are involved in the formation of septal junctions include SepJ, FraC and FraD (Flores *et al*., 2007; Merino-Puerto *et al.*, 2010; Nürnberg *et al.*, 2015; Ramos-León *et al.*, 2018). *Anabaena* mutants of the genes encoding these proteins show a filament fragmentation phenotype that may result from deregulated activity of the cell wall AmiC amidases that drill the nanopores in the septal peptidoglycan (Bornikoel *et al.*, 2017). The *sepJ* and *fraC fraD* mutants also show a decreased number of nanopores (Nürnberg *et al.*, 2015) and are impaired in the intercellular transfer of the fluorescent markers (Mullineaux *et al.*, 2008; Merino-Puerto *et al.*, 2011; Nürnberg *et al.*, 2015). Two types of septal junctions may be present in *Anabaena*, one related to SepJ and another related to FraC and FraD (Merino-Puerto *et al.*, 2011; Nürnberg *et al.*, 2015). Septal junctions that contain FraD and require FraC for full assembly have been recently visualized by cryoET (Weiss *et al.*, 2019). Because these junctions are still observed in a *sepJ* mutant, the structures responsible for specific *sepJ* intercellular communication phenotypes (Corrales-Guerrero *et al.*, 2015; Mariscal *et al.*, 2016; Rivers *et al.*, 2014) remain to be identified. Interestingly, a *sepJ fraC fraD* triple mutant still forms some nanopores (about 7 % the number in the wild type) and shows significant transfer of the fluorescent markers, about 30 to 50 % of wild-type transfer between nitrate-grown vegetative cells (Nürnberg *et al.*, 2015), suggesting that additional proteins may be involved in the formation of septal junctions.

HglK (All0813) is a complex protein that bears an N-terminal domain containing four transmembrane segments and a C-terminal domain that includes a fragment with 36 repeats of a pentapeptide of consensus sequence ADLSG (Fig. S1). This protein was identified as the product of a gene whose inactivation results in a Fox– phenotype (inability to grow fixing N_2

under oxic conditions) (Black *et al.*, 1995). The *hglK* mutant produces immature heterocysts that lack the Hgl layer, do not show rearranged intracellular membranes and lack the polar cyanophycin plugs. Heterocyst glycolipids are however synthesized in the mutant, and hence it was proposed that HglK is involved in Hgl transport or deposition of the Hgl envelope layer (Black *et al.*, 1995). An intriguing characteristic of the *hglK* mutant is that intercellular septa, those between vegetative cells as well as those between vegetative cells and heterocysts, are broader than in the wild type (Black *et al.*, 1995). Based on this observation, we asked whether HglK could be an additional protein related to the septal junctions in *Anabaena*.

Results

Subcellular localization of HglK

To investigate the subcellular localization of HglK, an *Anabaena* strain producing an HglK fusion to the green fluorescent protein (GFP) was prepared. Because the C-terminus of HglK is predicted to be periplasmic (Fig. S1), we used the superfolder GFP that can fold efficiently in the periplasm (Dinh and Bernhardt, 2011). An *Anabaena* strain with the *sf-gfp* gene added to the 3'end of *hglK* was constructed (Fig. S2). Probably because of low expression of the *hglK* gene (Black *et al.*, 1995), a low level of GFP fluorescence was observed even in filaments incubated without combined nitrogen, conditions that elicit an increased expression of *hglK* (Table S1). Nonetheless, HglK-sfGFP could be observed in the periphery of the cells (outside of the thylakoid's red fluorescence) and, prominently, at the intercellular septa, indicating that it is a cytoplasmic membrane protein with an increased polar localization (Fig. 1). In some intercellular septa, two spots of GFP fluorescence could be observed. In heterocysts, HglK-sfGFP was observed at the cell poles but also peripherally (Fig. 1). The strain producing the HglK-sfGFP showed, in different tests, no growth or weak growth under diazotrophic conditions (see Fig. S4 below), indicating that HglK-sfGFP was hardly functional and making it necessary to seek for additional data.

To obtain independent evidence of the subcellular localization HglK, *Anabaena* strains producing HglK with 6xHis or Strep II tags added to its C-terminus were constructed to perform immunolocalization analysis (Fig. S3). Whereas the strain producing HglK-6xHis could not grow diazotrophically, the strain producing HglK-Strep II did grow (Fig. S4), indicating that HglK-Strep II is functional. In the strain producing His-tagged HglK, discernible signals could be seen as small foci of fluorescence localized mainly at the intercellular septa and at heterocyst poles (Fig. 2A). In the strain producing Strep-tagged HglK, immunolabeling was again observed mainly at the intercellular septa or close to them (Fig. 2B). With both tagged proteins, two spots of labeling were frequently observed at the cell poles (double arrows in Fig. 2), reminiscent of double spots also observed with HglK-sfGFP (double arrows in Fig. 1). To get a better idea of the subcellular localization of HglK, the immunofluorescence spots observed in the septa or outside the septa were quantified using the wild type as a control of unspecific binding of the antibodies to the biological samples (Fig. 2, lower panels). About one septal spot and 0.2 non-septal spots per cell were counted for both HglK-6xHis and HglK-Strep II, whereas the wild type control showed in both cases about 0.1 septal and non-septal spots per cell. If the wild-type controls are subtracted, the number of immunofluorescence spots is about 7.5-fold higher in the septa than in the rest of the cell for both HglK-6xHis and HglK-Strep II. In summary, in spite of a low expression of the *hglK* gene (Black *et al.*, 1995), these results together with those obtained with HglK-sfGFP indicate that HglK is a protein of predominant localization at the intercellular septa in *Anabaena*.

Inactivation of hglK *in different mutant backgrounds*

To investigate aspects of the phenotype of an *hglK* mutant that were not addressed in the original description of this gene (Black *et al.*, 1995), we introduced an *hglK* deletion-insertion mutation (Δ*hglK*::C.K1) in wild-type *Anabaena* and in a deletion mutant of the *sepJ* gene (Δ*sepJ*), in a Δ*fraC* Δ*fraD* double mutant, and in a Δ*sepJ* Δ*fraC* Δ*fraD* triple mutant, producing strains CSSA1 (*hglK*), CSSA2 (*fraC fraD hglK*), CSSA3 (*sepJ hglK*) and CSSA12 (*fraC fraD*

sepJ hglK) (Fig. S5). As previously shown for an *hglK* mutant (Black *et al.*, 1995), and as expected for the strains bearing multiple mutations including Δ*hglK*::C.K1, none of these mutants could grow fixing N_2 under oxic conditions (Fig. S6). Nonetheless, consistent with the results of Black *et al.* (1995), our *hglK* mutant (strain CSSA1) produced heterocysts, which were about 5.4 % of total cells after 48 h of incubation in $BG11_0$ medium, whereas in the wild type heterocysts were about 7 % of total cells under the same conditions.

To study how active those heterocysts could be, nitrogenase activity was determined by the acetylene reduction assay under both oxic and anoxic conditions. The activity of strain CSSA1 was about 1.6 % and 3.7 % the activity of the wild type under oxic and anoxic conditions, respectively (Fig. S7). Therefore, in contrast to the *hglK* mutant described earlier that was reported to fix nitrogen microaerobically (although no quantitative data were shown; Black *et al.*, 1995), our *hglK* mutant only shows a marginal increase of nitrogenase activity when assayed under anoxic conditions, implying a defect in the production of this enzyme.

To investigate whether inactivation of *hglK* has any effect on the expression of genes activated at medium and late steps of heterocyst differentiation, *northern* analysis with probes of the *coxB2* and *nifH* genes was performed. The *cox2* operon encodes a heterocyst-specific cytochrome *c* oxidase that is expressed at mid differentiation (transcript detected at about 9 h; Valladares *et al.*, 2003), and the *nifHDK* genes encode the nitrogenase complex and are expressed late in differentiation (transcripts detected at about 18 h; Wei *et al.*, 1994). The expression of both the *cox2* operon and the *nifHDK* genes was substantially decreased in the *hglK* mutant as compared to the wild type (Fig. 3). After normalization with the *rnpB* control, the levels of the *cox2* operon transcript in the mutant were calculated to be about 15 and 19 % those of the wild type after 10 and 24 hours of nitrogen deprivation, respectively, and the levels of the *nifH* transcript in the mutant were about 8.5 % those of the wild type after 24 h of nitrogen deprivation. These results are consistent with detection of low levels of nitrogenase activity in the *hglK* mutant and indicate that inactivation of *hglK* impairs gene expression associated to heterocyst differentiation.

Mutants of genes such as *sepJ*, *fraC*, and *fraD* that encode septal proteins generally show a filament fragmentation phenotype (Bauer *et al.*, 1995; Flores *et al.*, 2007; Merino-Puerto *et al.*, 2010). Therefore, because the HglK protein appears to be localized at the intercellular septa, we investigated filament length in the *hglK* mutant. Strain CSSA1 produced shorter filaments than the wild type, and this was especially evident in BG11 medium, in which the wild type produced the highest proportion of long filaments (Fig. 4). When the Δ*hglK*::C.K1 mutation was introduced in the *sepJ*, *fraC* and *fraD* mutants, filament length was similar to (or not shorter than) that of the corresponding parental strain (Fig. S8). Hence, inactivation of *hglK* produces filament fragmentation but does not increase the fragmentation observed in the *sepJ*, *fraC* or *fraD* mutants.

Intercellular junctions and communication

Because of the broad intercellular septa present in the original *hglK* mutant (Black *et al.*, 1995), and because of the predominant septal localization of HglK (Figs. 1 and 2) and the filament fragmentation phenotype of our *hglK* mutant (Fig. 4), we investigated structures and functions related to intercellular communication. We first looked at nanopores in septal peptidoglycan disks from the *hglK* mutant and the wild type. The mutant had about 50 % the number of nanopores found in the wild type, and nanopore diameter was slightly larger in the mutant than in the wild type (Fig. 5). Thus, HglK appears to have a role of in the construction of mature septa.

We next looked at intercellular transfer of fluorescent markers studied by FRAP analysis. Because the expression of *hglK* is increased after nitrogen deprivation (Table S1), filaments incubated in the absence of combined nitrogen ($BG11_0$ medium) were used. Transfer of calcein between vegetative cells was decreased by inactivation of *sepJ*, *fraC* and *fraD* (Fig. 6A; see numerical data in Table S2), as previously described (Mullineaux *et al.*, 2008; Merino-Puerto *et al.*, 2010). Inactivation of *hglK* significantly decreased calcein transfer, but it did not decrease significantly transfer in the *fraC fraD*, *sepJ* or *fraC fraD sepJ* backgrounds beyond the

decrease caused by these mutations (Fig. 6A; Table S2). The negative effect of inactivation of *hglK* on molecular exchange between vegetative cells was corroborated by analyzing transfer of 5-carboxyfluorescein (5-CF), which was also significantly decreased in the mutant (Fig. 6B; Table S2). Thus, HglK is required for normal function of the septal junctions, but its effect is not additive to that of removal of SepJ or FraCD. In contrast to its negative effect on calcein transfer between vegetative cells, inactivation of *hglK* resulted in a significant increase of calcein transfer from vegetative cells to heterocysts (Fig. 6C; Table S2). This implies the presence of functional junctions in the septa between vegetative cells and heterocysts of the *hglK* mutant (see Discussion).

Subcellular localization of SepJ and FraD

The results shown in the previous section suggest a role of HglK in the septal junctions. We then investigated by immunofluorescence whether the Δ*hglK*::C.K1 mutation affected the subcellular localization of septal proteins SepJ and FraD. Immunofluorescence analysis was performed with antibodies raised against the coiled-coil domain of SepJ (Mariscal *et al.*, 2011) or against the extramembrane (periplasmic) fragment of FraD (Merino-Puerto *et al.*, 2011). Septal signals of SepJ were evident in the wild type and were missing from a negative control strain that lacks the *sepJ* gene, strain CSSA3 (Fig. 7A). In the *hglK* mutant, SepJ was localized at the intercellular septa like in the wild type. Labeling of FraD was unfortunately not as clear as that of SepJ. Nonetheless, FraD spots localized at the intercellular septa could be observed in the wild type that were missing from a *fraD* mutant control, strain CSSA2 (Fig. 7B). In the *hglK* mutant, FraD spots could be observed at the intercellular septa but also out of the septa (Fig. 7B). Quantification of immunofluorescence spots did not show, however, any significant difference between the *hglK* mutant and the wild type in the septal localization of FraD.

Discussion

In this work, we have shown that HglK is a protein predominantly localized in the septal regions of the filaments of *Anabaena*, and that inactivation of the *hglK* gene results in filament fragmentation, a decreased number of septal peptidoglycan nanopores and decreased activity of intercellular molecular transfer between vegetative cells. However, inactivation of *hglK* does not increase the effects on these parameters that result from inactivation of *sepJ* or *fraC* and *fraD*. Furthermore, inactivation of *sepJ* or *fraC* and *fraD* has a stronger effect on those parameters than inactivation of *hglK* (Nürnberg *et al.*, 2015). Hence, HglK might influence the formation of septal junctions rather than constitute an independent type of junctions. The recently visualized FraD-containing septal junctions evidently comprise additional proteins (Weiss *et al.*, 2019). Whether HglK could be a component of the septal junctions or solely contribute to their assembly remains to be investigated. In any case, HglK could be a structural component of the intercellular septa affecting the formation of septal junctions. In this context, the frequent observation of HglK double spots that are laterally, rather than centrally, localized in the septa (Figs. 1 and 2) is of interest. A role of HglK in the construction of mature septa is consistent with the original observation that inactivation of *hglK* results in the formation of broad intercellular septa (Black *et al.*, 1995).

Our results have shown that inactivation of *hglK* impairs calcein and 5-CF transfer between vegetative cells. In contrast, calcein transfer to heterocysts was increased significantly in the *hglK* mutant. Calcein transfer to the heterocysts appears to be specifically related to SepJ (Mariscal *et al.*, 2016), whose localization is unaltered in the *hglK* mutant (Fig. 7A). The positive effect of inactivation of *hglK* on calcein transfer to the heterocysts can be related to the lack, in the mutant, of cyanophycin plugs (Black *et al.*, 1995), which have been shown to restrict transfer of calcein into the heterocysts (Mullineaux *et al.*, 2008). Whether, additionally, HglK has a regulatory effect on the septal junctions that are functional between vegetative cells and heterocysts is unknown.

As described in the Introduction, HglK is a membrane protein with a predicted long pentapeptide-repeat fragment that is likely localized in the periplasm (Fig. S1B, C). As

predicted by Phyre2 (www.sbg.bio.ic.ac.uk/phyre2/), the pentapeptide-repeat fragment of HglK has a structure very similar to that of HetL (Ni *et al.*, 2009). Pentapeptide-repeat proteins adopt a highly regular four-sided, right-handed β helical structure (Fig. S1D) that might perform a structural function. There are as many as 32 pentapeptide-repeat proteins in *Anabaena*, and at least five of them bear signal peptides that may direct those proteins to the periplasm (Ni *et al.*, 2009). The limited effect of inactivation of *hglK* on the parameters that we have studied may reflect that, in *Anabaena*, other proteins have a role redundant with that of HglK. Indeed, inactivation or altered expression of some genes encoding pentapeptide-repeat proteins have been shown to affect filamentation or heterocyst formation related to intercellular molecular transfer in *Anabaena*. Thus, FraF is a pentapentide-repeat protein encoded in a cluster of genes (*fraC-fraD-fraE*←*fraF*, where the arrow indicates a change of orientation) that affect filament length (Merino-Puerto *et al.*, 2013), and HetL and PatL are pentapeptide-repeat proteins that affect heterocyst pattern formation (Liu and Golden, 2002; Liu and Wolk, 2011). Interestingly, whereas PatL and FraF are widely distributed in heterocystous cyanobacteria and HetL seems to have a more restricted distribution, HglK is universally present in these organisms suggesting an essential function (Table S3). Of further interest, PatL is a predicted membrane-anchored protein that likely has a topology very similar to that of HglK (Fig. S9, compare to Fig. S1). Whether PatL and HglK have somewhat associated or redundant functions remains to be investigated.

Because the *hglK* mutant was shown to synthesize heterocyst-specific glycolipids (Hgl) but not to deposit an Hgl layer, HglK was suggested to be involved in the export of Hgl or deposition of the Hgl layer (Black *et al.*, 1995). However, the transporter of Hgl to the outside of the outer membrane has now been identified as the ATP-driven efflux pump DevBCA/HgdD (Staron *et al.*, 2011). Here we have shown, on the other hand, that the *hglK* mutant is impaired in heterocyst differentiation, failing to express at normal levels some genes activated at intermediate and late steps of the differentiation process. It is possible, therefore, that rather than being specifically involved in Hgl export or deposition, HglK has a more general role in heterocyst differentiation, its inactivation resulting in a deficiency of several differentiation-

related processes. Because HglK appears to influence the formation of the septal junctions, impairment, in the *hglK* mutant, in the intercellular transfer of some compounds could be responsible for the phenotype of deficient differentiation. This would be similar to the situation in the *sepJ* mutant, in which heterocyst differentiation is aborted after synthesis of the heterocyst polysaccharide layer but before synthesis of Hgl (Flores *et al.*, 2007; Nayar *et al.*, 2007). SepJ appears to be involved in the intercellular transfer of the PatS morphogen and of a HetN-dependent regulator of heterocyst differentiation (Mariscal *et al.*, 2016; Rivers *et al.*, 2014), but the physiological compounds whose intercellular transfer may be affected by inactivation of *hglK* are currently unknown.

In summary, our results have shown that the pentapeptide-repeat protein HglK is involved in the formation of fully functional septal junctions and is needed for the differentiation of functional heterocysts in *Anabaena*. The function of a number of pentapeptide-repeat proteins in different aspects of heterocyst differentiation is intriguing and raise the possibility that some of those proteins are (at least partially) redundant for the formation of the septal junctions, which are complex entities that appear to include a number of different proteins.

Experimental procedures

Strains and growth conditions

Anabaena sp. strain PCC 7120 was grown axenically in BG11 medium (containing $NaNO_3$) or $BG11_0$ medium (free of combined nitrogen). In every case, ferric citrate replaced the ferric ammonium citrate used in the original recipe (Rippka *et al.*, 1979). For plates, medium was solidified with 1% separately autoclaved Difco agar. Cultures were grown at 30 ºC in the light (25 μmol photons m^{-2} s^{-1}), with shaking (80-90 rpm) for liquid cultures. Alternatively, cultures (referred to as bubbled cultures) were supplemented with 10 mM $NaHCO_3$ (BG11C or $BG11_0$C) and bubbled with a mixture of CO_2 and air (1 % v/v) in the light (50 to 75 μmol photons m^{-2} s^{-1}). For mutants described below, antibiotics were used at the following concentrations: neomycin

303 trisulfate salt hydrate (Nm) at 30 μg mL^{-1} for solid media and 15 μg mL^{-1} for liquid media;
304 streptomycin sulfate (Sm) and spectinomycin dihydrochloride pentahydrate (Sp), 5 μg mL^{-1} and
305 2.5 μg mL^{-1} each in solid and liquid media, respectively. DNA was isolated from *Anabaena* sp.
306 by the method of Cai and Wolk (1990). *Anabaena* strains CSVM34 (Δ*sepJ*; Mariscal *et al.*,
307 2011), CSVT22 (Δ*fraC* Δ*fraD*; Merino-Puerto *et al.*, 2011) and CSVM141 (Δ*sepJ* Δ*fraC*
308 Δ*fraD*; Nürnberg *et al.*, 2015) are marker-less mutants that have been described previously.
309 *Escherichia coli* DH5α was used for plasmid constructions, and strains HB101 and
310 ED8654 for conjugations with *Anabaena* strains. They were grown in LB medium,
311 supplemented when appropriate with antibiotics at standard concentrations (Ausubel *et al.*,
312 2014).
313
314 *Construction of mutants*
315 The genomic sequence of *Anabaena* is available (Kaneko *et al.*, 2001). Oligodeoxynucleotide
316 primers used in this work are shown in Table S4. The plasmid carrying fusion gene *hglK-sf-gfp*
317 (*all0813-sf-gfp*) was prepared as follows. A 671-bp fragment from the 3'-terminal part of *hglK*
318 was amplified by PCR using *Anabaena* DNA as template and primers all0813-15 (which lacks
319 the stop codon of the gene and contains a BsaI site in its 5' end) and all0813-14 (which contains
320 KpnI and HindIII sites in its 5' end), and the resulting fragment was cloned as a HindIII/BsaI-
321 ended fragment in HindIII/BsaI-digested pCSAL39 producing plasmid pCSSA12 that carries
322 the fusion of the *sf-gfp* gene to the 3' end of *hglK* (pCSAL39 is a pMBL-T-derived vector that
323 contains the *sf-gfp* gene, a sequence encoding a 4-Gly linker and a BsaI site in its 5' end). The
324 insert of pCSSA12 was corroborated by sequencing and the resulting fusion was transferred as a
325 KpnI-ended fragment to KpnI-digested pCSV3, which provides resistance to Sm and Sp
326 (Valladares *et al.*, 2011), producing pCSSA13 (Fig. S2). This plasmid, which bears the fusion of
327 the *sf-gfp* gene to the 3' end of *hglK* (including a sequence encoding a tetra-Gly linker), was
328 transferred to *Anabaena* wild type by triparental mating with selection for Sm^R Sp^R (Elhai *et al.*,
329 1997). Insertion into *hglK* and segregation of chromosomes carrying the fusion was tested by

PCR using template DNA from exconjugant clones and primers all0813-10 and gfp-8 for testing insertion of *sf-gfp*, and all0813-16 and all0813-10 for testing segregation of the mutated chromosomes. A clone bearing the *sf-gfp* fusion to *hglK* was named CSSA4 (*hglK-sf-gfp*) (Fig. S2).

To add a 6xHis tag to the C-terminus of HglK, a C-terminal fragment of *hglK* was amplified by PCR with *Anabaena* DNA as template and primers all0813-12 (which includes an EcoRI site at its 5' end) and all0813-13 (which includes a sequence encoding the 6xHis tag and an EcoRI site at its 5' end). This fragment was cloned into EcoRI-digested pCSV3 producing pCSSA11 (Fig. S3). To add a Strep-tag II to the C-terminus of HglK, a C-terminal fragment of *hglK* was amplified by PCR with *Anabaena* DNA as template and primers all0813-24 (which includes an EcoRI site at its 5' end) and all0813-25 (which includes a sequence encoding the Strep-tag II and an EcoRI site at its 5' end). This fragment was cloned into EcoRI-digested pCSV3 producing pCSSA30 (Fig. S3). Plasmids pCSSA11 and pCSSA30 were corroborated by sequencing and transferred to *Anabaena* wild type by triparental mating with selection for Sm^R Sp^R (Elhai *et al.*, 1997). Incorporation of the constructs into the *hglK* region was tested by PCR analysis (Fig. S3), and correct clones were chosen and named CSSA7 (*hglK-6xHis*) and CSSA18 (*hglK-Strep II*).

For construction of the *hglK* mutant, fragments of the upstream and downstream regions of *hglK* (ORF *all0813*) were amplified by PCR with *Anabaena* DNA as template and the primers shown in Fig. S5 which are flanked by SacI and XbaI sites. Those fragments were joined together at the XbaI sites and corroborated by sequencing. The Nm-resistance cassette C.K1 (which bears the *npt* gene and its own natural promoter; Elhai and Wolk, 1988) was inserted into the XbaI site, and the whole fragment was cloned into SacI-digested pCSRO (Merino-Puerto *et al.*, 2013), which carries an Sm/Sp-resistance determinant and the *sacB* gene for positive selection (Cai and Wolk, 1990), producing plasmid pCSSA6 (Fig. S5). Plasmid pCSSA6 was transferred by triparental conjugation (Elhai *et al.*, 1997) to *Anabaena* wild type and mutants CSVM34, CSVT22 and CSVM141 with selection for resistance to Sm/Sp. Clones resistant to sucrose that lacked the vector portion of pCSSA6 were selected, corroborated by

PCR analysis (Fig. S5) and named CSSA1 (Δ*hglK*::C.K1), CSSA2 (Δ*fraC* Δ*fraD* Δ*hglK*::C.K1), CSSA3 (Δ*sepJ* Δ*hglK*::C.K1) and CSSA12 (Δ*fraC* Δ*fraD* Δ*sepJ* Δ*hglK*::C.K1).

Growth tests, nitrogenase activity and northern blot analysis

Chlorophyll *a* (Chl) content of the cultures was determined by the method of Mackinney (1941). For growth tests on solid media, cultures grown in BG11 medium (with Nm for the *hglK* mutants) were harvested and washed three times with $BG11_0$ medium. Dilutions were prepared in $BG11_0$ medium and samples of 8 µl of the resulting suspensions were spotted on agar plates with different nitrogen sources that were incubated at 30 °C in the light (25 µmol photons m^{-2} s^{-1}). The growth rate constant ($\mu=[\ln 2]/t_d$, where t_d is the doubling time) was calculated from the increase in $OD_{750\ nm}$ of shaken liquid cultures. Cultures were inoculated with an amount of cells containing 0.1 µg Chl mL^{-1} and the suspensions of filaments were carefully homogenized with a pipette before taking the samples.

Nitrogenase activity was determined by the acetylene reduction assay under oxic and anoxic conditions as described previously (Burnat and Flores, 2014). Cells grown in 25 to 50 mL of BG11 medium were washed with $BG11_0$ medium, inoculated at 1 µg Chl mL^{-1} and incubated 48 h without combined nitrogen ($BG11_0$ medium) under growth conditions and used in the acetylene reductions assays.

Total RNA was extracted from 200-mL bubbled cultures by a procedure described previously (Luque *et al.*, 2002). For each sample, 10 µg RNA was resolved in a formaldehyde-containing 1% agarose gel, transferred onto Genescreen Plus nylon membranes (PerkinElmer), and hybridized to radioactive DNA probes of *coxB2* and *nifH* generated with primers coxB2-5/coxB2-6 and nifH-7120-1/nifH-7120-4, respectively. These DNA fragments were labelled with [α-^{32}P]dCTP by using the Klenow fragment (Fermentas). Images of hybridized membranes were obtained and the signals were quantified with a Cyclone Storage Phosphor system (PerkinElmer). As a control of RNA loading and transfer efficiency, the filters were hybridized

with a probe of the RNase P RNA gene (*rnpB*) from *Anabaena* generated with primers rnpB-4 and rnpB-5 (Vioque, 1997).

Standard and confocal microscopy

To determine filament length, filaments grown in BG11 medium (in the presence of Nm for the mutants) were harvested, washed three times with nitrogen-free ($BG11_0$) medium and resuspended at 1 µg Chl mL^{-1} in BG11 or $BG11_0$ medium without antibiotics. After 24, 48 or 72 h of incubation at 30ºC in the light, samples were set atop BG11 or $BG11_0$ solid medium, respectively, and visualized by standard light microscopy. The percentage of heterocysts was determined by counting about 2,000 cells of the wild type and about 3,000 cells of the *hglK* mutant (strain CSSA1).

For confocal microscopy of strains producing the sfGFP, filaments grown in bubbled BG11C medium (in the presence of Sm + Sp for the mutants) were harvested, washed three times with $BG11_0$C medium, resuspended at 3 µg Chl mL^{-1} in $BG11_0$C medium (without antibiotics), and incubated for 24 h as bubbled cultures. Samples were set atop $BG11_0$ solid medium and visualized using a PlanApo 63X / 1.40 oil DIC M27 immersion objective attached to a Zeiss LSM 7 duo confocal laser-scanning microscope. GFP was excited using 488-nm laser irradiation. Fluorescence emission was collected in a spectral detector from 504 to 727 nm (approximately 10-nm windows) and pixels were analyzed to coincide with GFP or Chl fluorescence. The images shown in Fig. 1 comprise GFP and Chl fluorescence.

Immunofluorescence localization of proteins

Filaments grown in BG11 medium (in the presence of antibiotics for the mutants) were harvested, washed three times with nitrogen-free ($BG11_0$) medium and resuspended at 1 µg Chl mL^{-1} in $BG11_0$ medium without antibiotics. After 24 or 48 h of incubation at 30ºC in the light, cells from 5 mL of liquid cultures were collected by centrifugation, placed atop a poly-L-lysine pre-coated microscope slide and covered with a 45-µm pore-size Millipore filter. The filter was

411 removed and the slide was let dry at room temperature and, then, immersed in 70% ethanol
412 at -20ºC for 45 min and dried 15 min at room temperature. The cells were washed twice (2 min
413 each time, room temperature) by covering the slide with PBS-T (PBS supplemented with 0.05%
414 Tween-20). Subsequently, the slides were treated with a blocking buffer (5% milk powder in
415 PBS-T) for 30 min. To study the localization of SepJ or FraD, the cells on the slides were
416 incubated for 90 min with anti-SepJ-CC antibodies (Mariscal *et al.*, 2011) or anti-FraD
417 antibodies (Merino-Puerto *et al.*, 2011) diluted 1:200 in blocking buffer, washed three times
418 with PBS-T, incubated 45 min in the dark with anti-rabbit antibody conjugated to fluorescein
419 isothiocyanate (FITC) (Sigma, 1:500 dilution in PBS-T) and washed three times with PBS-T.
420 After dried, several drops of FluorSave (Calbiochem) were added atop, covered with a coverslip
421 and sealed with nail lacquer. To study the localization of HglK fused to 6xHis or Strep II tag,
422 the cells on the slides were incubated for 45 min with Penta-His™ Alexa Fluor® 488 conjugate
423 (Qiagen Gmbh, Germany) or StrepMAB-Classic (specific for Strep-tag II) conjugated to
424 Chromeo™ 488 (Iba Gmbh, Germany), diluted 1:200 or 1:250, respectively, in blocking buffer.
425 Fluorescence was imaged using a Leica DM6000B fluorescence microscope and an ORCA-ER
426 camera (Hamamatsu). Fluorescence was monitored using a FITC L5 filter (excitation, band-pass
427 [BP] 480/40 filter; emission, BP 527/30 filter), and images were analyzed with ImageJ software
428 (http://imagej.nih.gov/ij).
429

430 *Intercellular transfer of calcein and 5-CF*

431 For calcein and 5-CF transfer assays (FRAP analysis), calcein and 5-CF staining were
432 performed as previously reported (Mullineaux *et al.*, 2008; Merino-Puerto *et al.*, 2011). Cell
433 suspensions were spotted onto agar and placed in a temperature-controlled sample holder with a
434 glass cover slip on top. All measurements were carried out at 30 °C. For both calcein and 5-CF,
435 cells were imaged with a Leica HCX PL Apo 63x, 1.4-NA oil immersion objective attached to a
436 Leica TCS SP2 confocal laser-scanning microscope with a 488-nm line argon laser as the
437 excitation source. Fluorescent emission was monitored by collection across windows of 500 to

520 nm and a 150-µm pinhole. After an initial image was recorded, the bleach was carried out by an automated FRAP routine as previously reported (Mullineaux *et al.*, 2008). For FRAP data analysis, kinetics of transfer of the fluorescent tracer was quantified and the recovery constant, *R*, was calculated as previously described (Nieves-Morión *et al.*, 2017).

Electron microscopy

Filaments grown in BG11 medium (with Nm for the *hglK* mutant) to about 3 to 4 µg Chl mL^{-1} were washed and incubated in $BG11_0$ medium for 48 h. The filaments were then harvested by centrifugation and the sacculi were isolated and analyzed as described previously (Lehner *et al*., 2013; Nürnberg *et al*., 2015). The purified sacculi were deposited on formvar/carbon film coated copper grids, and stained with 1% (w/v) uranyl acetate. All the samples were examined with a ZEISS LIBRA 120 PLUS electron microscope at 120 kV.

Acknowledgements

We thank Antonia Herrero (CSIC, Seville) and Enrico Schleiff (Goethe Universität, Frankfurt) for critically reading the manuscript, and Ana Valladares (CSIC, Seville) for help with the *northern* analysis. Work was supported by grant number BFU2017-88202-P from the Spanish Government co-financed by the European Regional Development Fund. S.A. was supported by a Formación del Personal Investigador (FPI) fellowship/contract from the Spanish Government.

Data on this article are available on request from the authors.

Conflict of interest

The authors declare that they have no conflict of interest.

Author Contributions

SA designed research, constructed mutants, and acquired and analyzed data; EF conceived the

study, designed research, analyzed data and wrote the manuscript.

References

Ausubel, F.M., Brent, R., Kingston, R.E., Moore, D.D., Seidman, J.G., Smith, J.A., and Struhl, K. (2014) Current Protocols in Molecular Biology. New York: *Greene Publishing and Wiley-Interscience.*

Bauer, C.C., Buikema, W.J., Black, K., and Haselkorn, R. (1995) A short-filament mutant of *Anabaena* sp. strain PCC 7120 that fragments in nitrogen-deficient medium. *J Bacteriol* **177**(6): 1520-1526.

Black, K., Buikema, W.J., and Haselkorn, R. (1995) The *hglK* gene is required for localization of heterocyst-specific glycolipids in the cyanobacterium *Anabaena* sp. strain PCC 7120. *J Bacteriol* **177**(22): 6440-6448.

Bornikoel, J., Carrión, A., Fan, Q., Flores, E., Forchhammer, K., Mariscal, V., Mullineaux, C.W., Perez, R., Silber, N., Wolk, C.P., and Maldener, I. (2017) Role of two cell wall amidases in septal junction and nanopore formation in the multicellular cyanobacterium *Anabaena* sp. PCC 7120. *Front Cell Infect Microbiol* **7**: 386 (doi: 10.3389/fcimb.2017.00386).

Burnat, M., and Flores, E. (2014) Inactivation of agmatinase expressed in vegetative cells alters arginine catabolism and prevents diazotrophic growth in the heterocyst-forming cyanobacterium *Anabaena*. *MicrobiologyOpen* **3**(5): 777-792.

Cai, Y., and Wolk, C.P. (1990) Use of a conditionally lethal gene in *Anabaena* sp. strain PCC 7120 to select for double recombinants and to entrap insertion sequences. *J Bacteriol* **172**: 3138-3145.

Corrales-Guerrero, L., Tal, A., Arbel-Goren, R., Mariscal, V., Flores, E., Herrero, A., and Stavans, J. (2015) Spatial fluctuations in expression of the heterocyst differentiation regulatory gene *hetR* in *Anabaena* filaments. *PLoS Genet* 11(4): e1005031.

Dinh, T., and Bernhardt, T.G. (2011) Using superfolder green fluorescent protein for periplasmic protein localization studies. *J Bacteriol* **193**(18): 4984-4987.

Elhai, J., and Wolk, C.P. (1988) A versatile class of positive-selection vectors based on the nonviability of palindrome-containing plasmids that allows cloning into long polylinkers. *Gene* **68:** 119-138.

Elhai, J., and Wolk, C.P. (1990) Developmental regulation and spatial pattern of expression of the structural genes for nitrogenase in the cyanobacterium *Anabaena. EMBO J* **9**(10): 3379-88.

Elhai, J., Vepritskiy, A., Muro-Pastor, A.M., Flores, E., and Wolk, C.P. (1997) Reduction of conjugal transfer efficiency by three restriction activities of *Anabaena* sp. strain PCC 7120. *J Bacteriol* **179:** 1998-2005.

Ermakova, M., Battchikova, N., Richaud, P., Leino, H., Kosourov, S., Isojärvi, J., Peltier, G., Flores, E., Cournac, L., Allahverdiyeva, Y., and Aro, E.-M. (2014) Heterocyst-specific flavodiiron protein Flv3B enables oxic diazotrophic growth of the filamentous cyanobacterium *Anabaena* sp. PCC 7120. *Proc Natl Acad Sci USA* **111**(30): 11205-11210.

Flores, E., Pernil, R., Muro-Pastor, A.M., Mariscal, V., Maldener, I., Lechno-Yossef, S., Fan, Q., Wolk, C.P., and Herrero, A. (2007) Septum-localized protein required for filament integrity and diazotrophy

in the heterocyst-forming cyanobacterium *Anabaena* sp. strain PCC 7120. *J Bacteriol* **189:** 3884-3890.

Flores, E., Nieves-Morión, M., and Mullineaux, C.W. (2019) Cyanobacterial septal junctions: properties and regulation. *Life (Basel)* **9**: 1 (doi:10.3390/life9010001).

Flores E, Picossi S, Valladares A, Herrero A. (2019) Transcriptional regulation of development in heterocyst-forming cyanobacteria. *Biochim Biophys Acta Gene Regul Mech* **1862**: 673-684.

Hahn, A., and Schleiff, E. (2014) The cell envelope. In *The Cell Biology of Cyanobacteria*. Flores, E. and Herrero, A. (eds.). Norfolk, UK: Caister Academic Press. pp. 29-87.

Herrero, A., Stavans, J., and Flores, E. (2016) The multicellular nature of filamentous heterocyst forming cyanobacteria. *FEMS Microbiol Rev* **40**: 831-854.

Kaneko, T., Nakamura, Y., Wolk, C.P., Kuritz, T., Sasamoto, S., Watanabe, A., Iriguchi, M., Ishikawa, A., Kawashima, K., Kimura, T., Kishida, Y., Kohara, M., Matsumoto, M., Matsuno, A., Muraki, A., Nakazaki, N., Shimpo, S., Sugimoto, M., Takazawa, M., Yamada, M., Yasuda, M., and Tabata, S. (2001) Complete genomic sequence of the filamentous nitrogen-fixing cyanobacterium *Anabaena* sp. strain PCC 7120. *DNA Res* **8:** 205-213.

Lehner, J., Berendt, S., Dörsam, B., Pérez, R., Forchhammer, K., and Maldener, I. (2013) Prokaryotic multicellularity: a nanopore array for bacterial cell communication. *FASEB J* **27:** 2293-30.

Liu, D., and Golden, J.W. (2002) *hetL* overexpression stimulates heterocyst formation in *Anabaena* sp. strain PCC 7120. *J Bacteriol* **184**(24): 6873-6881.

Liu, J., and Wolk, C.P. (2011) Mutations in genes *patA* and *patL* of *Anabaena* sp. strain PCC 7120 result in similar phenotypes, and the proteins encoded by those genes may interact. *J Bacteriol* **193**(21): 6070-6074.

Luque, I., Contreras, A., Zabulon, G., Herrero, A., and Houmard, J. (2002) Expression of the glutamyl-tRNA synthetase gene from the cyanobacterium *Synechococcus* sp. PCC 7942 depends on nitrogen availability and the global regulator NtcA. *Mol Microbiol* **46**(4): 1157-67.

Mackinney, G. (1941) Absorption of light by chlorophyll solutions. *J Biol Chem* **140**: 315-322.

Mariscal, V., Herrero, A., Nenninger, A., Mullineaux, C.W., and Flores, E. (2011) Functional dissection of the three-domain SepJ protein joining the cells in cyanobacterial trichomes. *Mol Microbiol* **79:** 1077-1088.

Mariscal, V., Nürnberg, D.J., Herrero, A., Mullineaux, C.W., and Flores, E. (2016) Overexpression of SepJ alters septal morphology and heterocyst pattern regulated by diffusible signals in *Anabaena*. *Mol Microbiol* **101**(6): 968-981.

Merino-Puerto, V., Mariscal, V., Mullineaux, C.W., Herrero, A., and Flores, E. (2010) Fra proteins influencing filament integrity, diazotrophy and localization of septal protein SepJ in the heterocyst-forming cyanobacterium *Anabaena* sp. *Mol Microbiol* **75:** 1159-1170.

Merino-Puerto, V., Schwarz, H., Maldener, I., Mariscal, V., Mullineaux, C.W., Herrero, A., and Flores, E. (2011) FraC/FraD-dependent intercellular molecular exchange in the filaments of a heterocyst-forming cyanobacterium, *Anabaena* sp. *Mol Microbiol* **82:** 87-98.

539 Merino-Puerto, V., Herrero, A., and Flores, E. (2013) Cluster of genes that encode positive and negative
540 elements influencing filament length in a heterocyst-forming cyanobacterium. *J Bacteriol* **195**(17):
541 3957-3966.
542 Mullineaux, C.W., Mariscal, V., Nenninger, A., Khanum, H., Herrero, A., Flores, E., and Adams, D.G.
543 (2008) Mechanism of intercellular molecular exchange in heterocyst-forming cyanobacteria. *EMBO J*
544 **27:** 1299-1308.
545 Nayar, A.S., Yamaura, H., Rajagopalan, R., Risser, D.D., and Callahan, S.M. (2007) FraG is necessary
546 for filament integrity and heterocyst maturation in the cyanobacterium *Anabaena* sp. strain PCC 7120.
547 *Microbiology* **153:** 601-603.
548 Ni, S., Sheldrick, G.M., Benning, M.M., and Kennedy, M.A. (2009) The 2A resolution crystal structure
549 of HetL, a pentapeptide repeat protein involved in regulation of heterocyst differentiation in the
550 cyanobacterium *Nostoc* sp. strain PCC 7120. *J Struct Biol* **165**(1):47-52.
551 Nieves-Morión, M., Lechno-Yossef, S., López-Igual, R., Frías, J.E., Mariscal, V., Nürnberg, D.J.,
552 Mullineaux, C.W., Wolk, C.P, and Flores, E. (2017) Specific glucoside transporters influence septal
553 structure and function in the filamentous, heterocyst-forming cyanobacterium *Anabaena* sp. strain
554 PCC 7120. *J Bacteriol* **199**(7): e00876-16.
555 Nürnberg, D.J., Mariscal, V., Bornikoel, J., Nieves-Morión, M., Krauß, N., Herrero, A., Maldener, I.,
556 Flores, E., and Mullineaux, C.W. (2015) Intercellular diffusion of a fluorescent sucrose analog via the
557 septal junctions in a filamentous cyanobacterium. *mBio* **6**(2): e02109.
558 Pratte, B.S., and Thiel, T. (2016) Homologous regulators, CnfR1 and CnfR2, activate expression of two
559 distinct nitrogenase gene clusters in the filamentous cyanobacterium *Anabaena variabilis* ATCC
560 29413. *Mol Microbiol* **100**: 1096–1109.
561 Ramos-León, F., Arévalo, S., Mariscal, V., and Flores, E. (2018) Specific mutations in the permease
562 domain of septal protein SepJ differentially affect functions related to multicellularity in the
563 filamentous cyanobacterium *Anabaena*. *Microb Cell* **5**(12): 555-565.
564 Rippka, R., Deruelles, J., Waterbury, J.B., Herdman, M., and Stanier, R.Y. (1979) Generic assignments,
565 strain histories and properties of pure cultures of cianobacteria. *J Gen Microbiol* **111**: 1-61.
566 Rivers, O.S., Videau, P., and Callahan, S.M. (2014) Mutation of *sepJ* reduces the intercellular signal
567 range of a hetN-dependent paracrine signal, but not of a patS-dependent signal, in the filamentous
568 cyanobacterium *Anabaena* sp. strain PCC 7120. *Mol Microbiol* 94(6): 1260-1271.
569 Staron, P., Forchhammer, K., and Maldener, I. (2011) Novel ATP-driven pathway of glycolipid export
570 involving TolC protein. *J Biol Chem* **286**(44): 38202-38210.
571 Valladares, A., Herrero, A., Pils, D., Schmetterer, G., and Flores, E. (2003) Cytochrome *c* oxidase genes
572 required for nitrogenase activity and diazotrophic growth in *Anabaena* sp. PCC 7120. *Mol Microbiol*
573 **47**(5): 1239-1249.
574 Valladares, A., Rodríguez, V., Camargo, S., Martínez-Noël, G.M.A., Herrero, A., and Luque, I. (2011)
575 Specific role of the cyanobacterial PipX factor in the heterocysts of *Anabaena* sp. strain PCC 7120. *J*
576 *Bacteriol* **193**: 1172-1182.

Vioque, A. (1997) The RNase P RNA from cyanobacteria: short tandemly repeated repetitive (STRR) sequences are present within the RNase PRNA gene in heterocyst-forming cyanobacteria. *Nucleic Acids Res* **25**: 3471–3477.

Wei, T.F., Ramasubramanian, T.S., and Golden, J.W. (1994) *Anabaena* sp. strain PCC 7120 *ntcA* gene required for growth on nitrate and heterocyst development. *J Bacteriol* **176**(15): 4473-4482.

Weiss, G.L., Kieninger, A.K., Maldener, I., Forchhammer, K., and Pilhofer, M. (2019) Structure and Function of a Bacterial Gap Junction Analog. *Cell* **178**(2): 374-384.

Wilk, L., Strauss, M., Rudolf, M., Nicolaisen, K., Flores, E., Kühlbrandt, W., and Schleiff, E. (2011) Outer membrane continuity and septosome formation between vegetative cells in the filaments of *Anabaena* sp PCC 7120. *Cell Microbiol* **13:** 1744-1754.

Wolk, C.P. (1996) Heterocyst formation. *Annu Rev Genet* **30:** 59–78.

590 **Figure legends**

591

592 Fig. 1. Subcellular localization of HglK-sfGFP. Confocal microscopy of *Anabaena* wild type
593 (PCC 7120) and strain CSSA4 that produces a fusion of superfolder GFP to the C-terminus of
594 HglK (*hglK-sf-gfp*). Filaments are from cultures incubated for 24 h in bubbled $BG11_0C$
595 medium. An overlay of GFP fluorescence and cyanobacterial autofluorescence is shown for
596 each strain. Some intercellular septa in which the GFP fluorescence is clearly observed are
597 indicated by arrows; double-opposite arrows indicate intercellular septa that are examples where
598 two spots are observed. het, heterocyst. Size bars, 5 µm.

599

600 Fig. 2. Subcellular localization of 6xHis- and Strep II-tagged HglK. (A) Immunofluorescence
601 analysis of *Anabaena* wild type (PCC 7120, negative control) or strain CSSA7 that produces the
602 HglK protein with a C-terminal 6xHis tag. Filaments incubated for 48 h in $BG11_0$ medium were
603 prepared and subjected to immunofluorescence analysis with anti-His-tag antibodies as
604 described in Experimental procedures. No signal is observed at the vegetative cells in the
605 bottom panel because the filament was focused to see the signals at the heterocyst (het). (B)
606 Immunofluorescence analysis of *Anabaena* wild type (PCC 7120, negative control) or strain
607 CSSA18 that produces the HglK protein with a C-terminal Strep II tag. Filaments incubated for
608 24 h in $BG11_0$ medium were prepared and subjected to immunofluorescence analysis with anti-
609 Strep-tag antibodies as described in Experimental procedures. Solid single arrows point to some
610 immunofluorescence spots localized at intercellular septa; double-opposite arrows indicate two
611 spots frequently observed in the cellular regions close to the intercellular septa; the dotted arrow
612 indicates an example of an immunofluorescence spot localized outside of the septal region.
613 Histograms in the lower part show number of immunofluorescence spots counted in the septal
614 regions (right columns, orange) or outside the septal regions (left columns, blue) in the strains
615 producing the HglK tagged proteins or the wild type (PCC 7120) as a negative control. Number
616 of cells analyzed were: for the His-tag antibodies, 115 (CSSA18) and 99 (PCC 7120); for the
617 Strep-tag antibodies, 111 (CSSA7) and 136 (PCC 7120). Size bars, 10 µm.

618

619 Fig. 3. Expression of the *cox2* and *nifHDK* gene clusters in *Anabaena* wild type and the *hglK*
620 mutant. *Northern* blot analysis with RNA isolated from cultures grown in bubbled BG11C
621 medium (supplemented with Nm for the *hglK* mutant) and incubated for 10 or 24 h in bubbled
622 $BG11_0C$ medium (without antibiotics). (A) A probe of the *coxB2* gene was used. Note the
623 presence of signals corresponding to the *cox2* operon transcript (about 3.7 kb; Valladares *et al.*,
624 2003). (B) A probe of the *nifH* gene was used. Note the presence of *nifHDK* (about 4.7 kb),
625 *nifHD* (about 2.8 kb), and *nifH* (about 1.1 kb) transcripts (Wei *et al*., 1994). Hybridization with
626 a probe of the *rnpB* gene was used as a loading and transfer control.

Fig. 4. Filament length in the *hglK* mutant. Cells of strain CSSA1 (Δ*hglK*::C.K1) and the wild type (PCC 7120) were grown in BG11 medium (in the presence of Nm for the mutant) and incubated in BG11 (top) or $BG11_0$ (bottom) medium (without antibiotics) for the indicated times. Samples were taken with great care to prevent disruption, and the number of cells per filament was determined in 100 to 120 filaments for each strain. The color codes on the right indicate number of cells per filament. For each growth condition, the distribution of filaments in the mutant was compared to that of the wild type using the Chi square test ($p < 10^{-8}$ in all cases).

Fig. 5. Nanopores in septal peptidoglycan disks of wild-type *Anabaena* and the *hglK* mutant. Cells were grown in BG11 medium (in the presence of Nm for the mutant), incubated in $BG11_0$ medium in the absence of antibiotics for 48 h and used for isolation of peptidoglycan and visualization by transmission electron microscopy as described in Experimental procedures. n, number of septal peptidoglycan disks analyzed to count nanopores or nanopores measured, respectively. Student's *t* test *p* (WT vs. mutant) indicated in each case.

Fig. 6. Effect of the Δ*hglK*::C.K1 mutation on the intercellular transfer of fluorescent markers in different genetic backgrounds (box-plot representations). (A) Calcein transfer between vegetative cells of the *hglK* mutant in the indicated genetic background. (B) 5-Carboxyfluorescein (5-CF) transfer between vegetative cells. (C) Calcein transfer from vegetative cells to heterocysts. Cells were grown in BG11 medium (in the presence of Nm for the *hglK* mutant), incubated for 48 h in $BG11_0$ medium without antibiotics, and used in FRAP analysis as described in Experimental procedures. Data are presented as the recovery rate constant, *R*. The number of filaments analyzed is indicated in parenthesis for each strain. Mann-Whitney U test analysis of *hglK* vs. indicated genetic background was performed, and *p* is indicated in each case. (See numerical data in supplementary Table S2.)

Fig. 7. Subcellular localization of SepJ and FraD in the *hglK* mutant. Filaments from the indicated strains incubated for 24 h in $BG11_0$ medium were used in immunofluorescence analysis with antibodies raised against the coiled-coil domain of SepJ (A) or against the extramembrane fragment of FraD (B). White arrows point to some SepJ (A) and FraD (B) spots at intercellular septa; yellow arrows point to some FraD spots outside of the intercellular septa in the *hglK* mutant. Size bars, 10 μm.

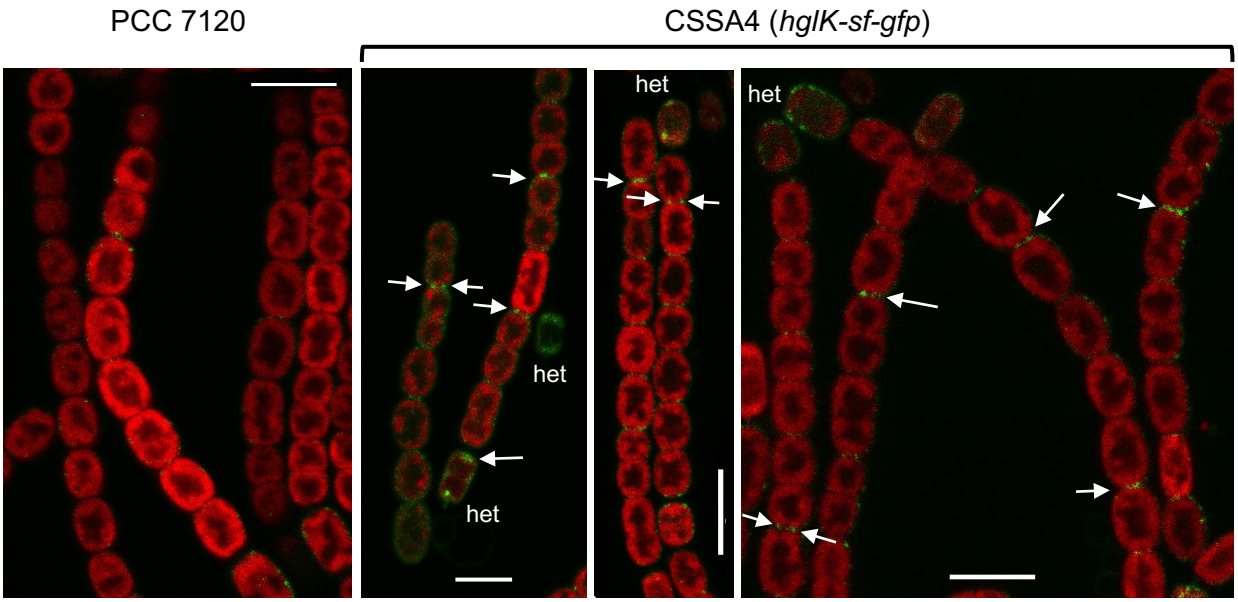
PCC 7120
CSSA4 (*hglK-sf-gfp*)
het
het
het
het

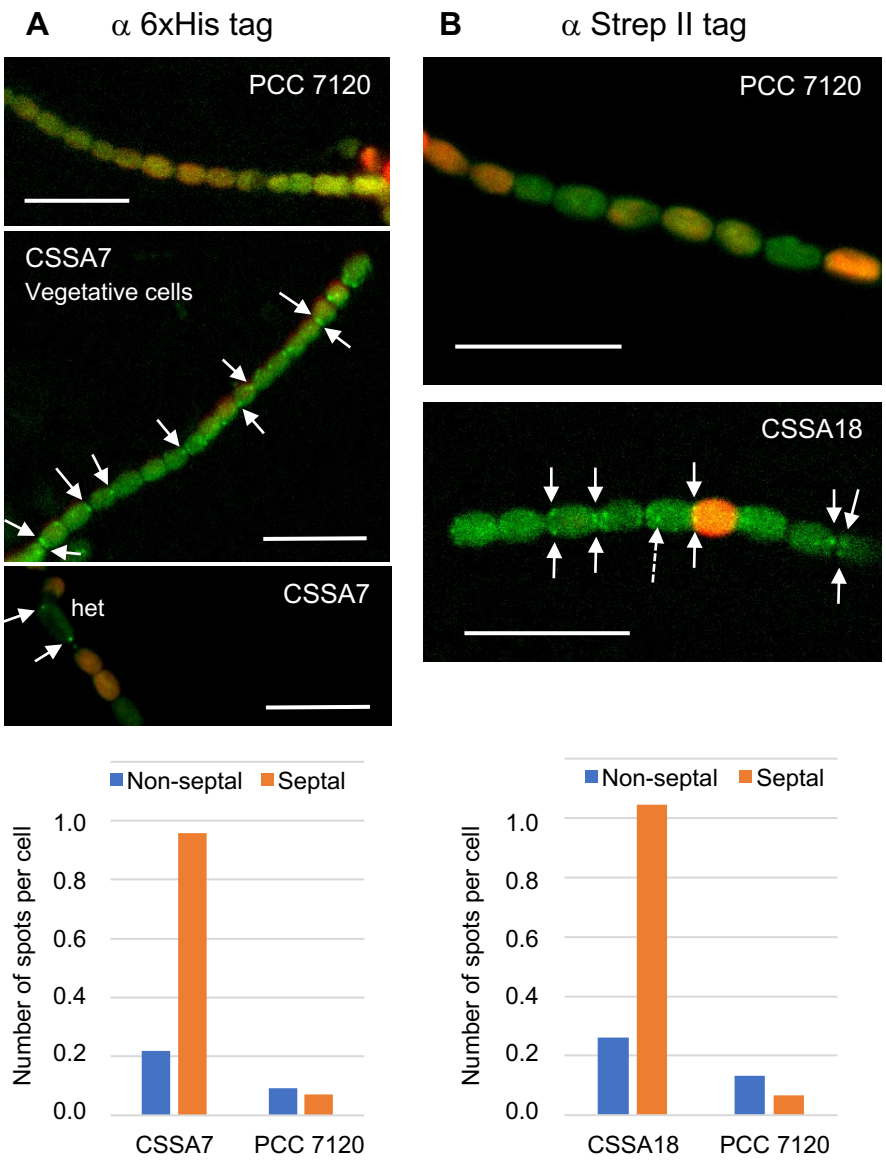
A
α 6xHis tag
PCC 7120
CSSA7
Vegetative cells
het
CSSA7
B
α Strep II tag
PCC 7120
CSSA18
Non-septal
Septal
Number of spots per cell
1.0
0.8
0.6
0.4
0.2
0.0
CSSA7
PCC 7120
Non-septal
Septal
Number of spots per cell
1.0
0.8
0.6
0.4
0.2
0.0
CSSA18
PCC 7120

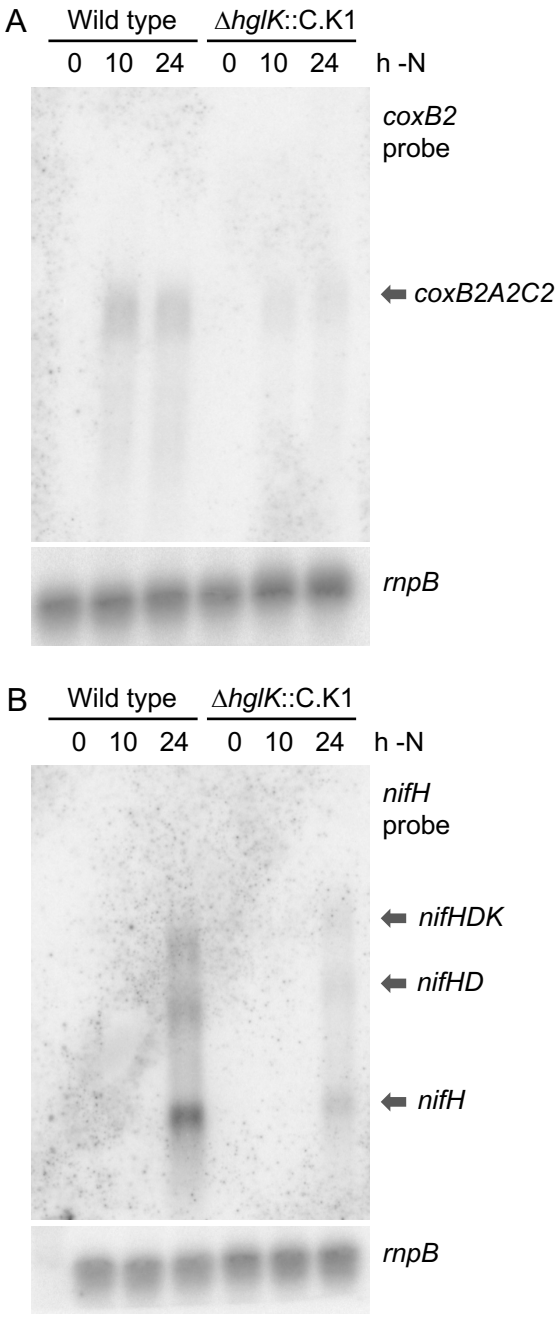
A
Wild type
ΔhglK::C.K1
0 10 24 0 10 24 h -N
coxB2
probe
coxB2A2C2
rnpB
B
Wild type
ΔhglK::C.K1
0 10 24 0 10 24 h -N
nifH
probe
nifHDK
nifHD
nifH
rnpB

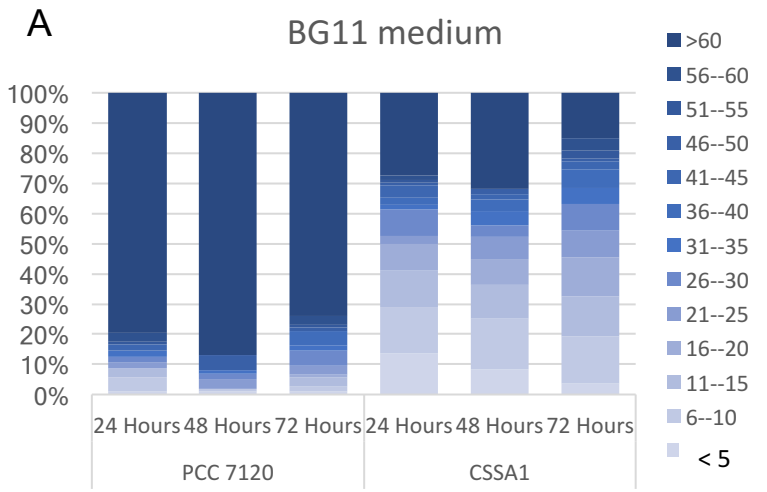
A
BG11 medium
100%
90%
80%
70%
60%
50%
40%
30%
20%
10%
0%
24 Hours
48 Hours
72 Hours
24 Hours
48 Hours
72 Hours
PCC 7120
CSSA1
>60
56--60
51--55
46--50
41--45
36--40
31--35
26--30
21--25
16--20
11--15
6--10
< 5

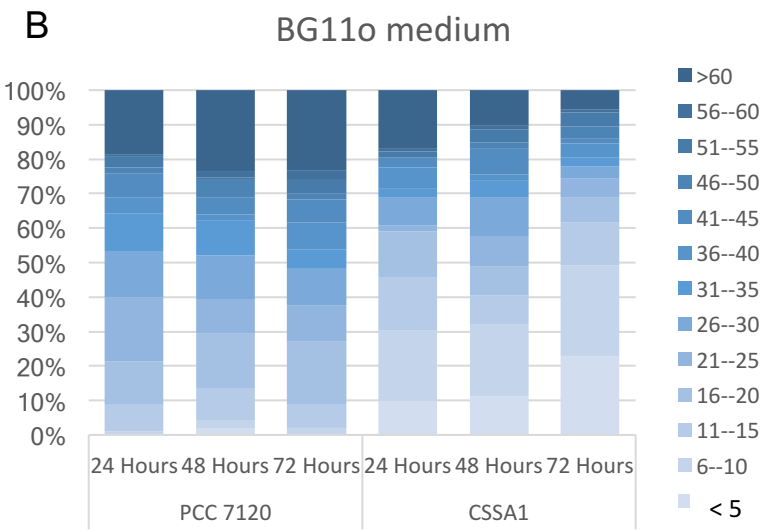
B
BG11o medium
100%
90%
80%
70%
60%
50%
40%
30%
20%
10%
0%
24 Hours
48 Hours
72 Hours
24 Hours
48 Hours
72 Hours
PCC 7120
CSSA1
>60
56--60
51--55
46--50
41--45
36--40
31--35
26--30
21--25
16--20
11--15
6--10
< 5

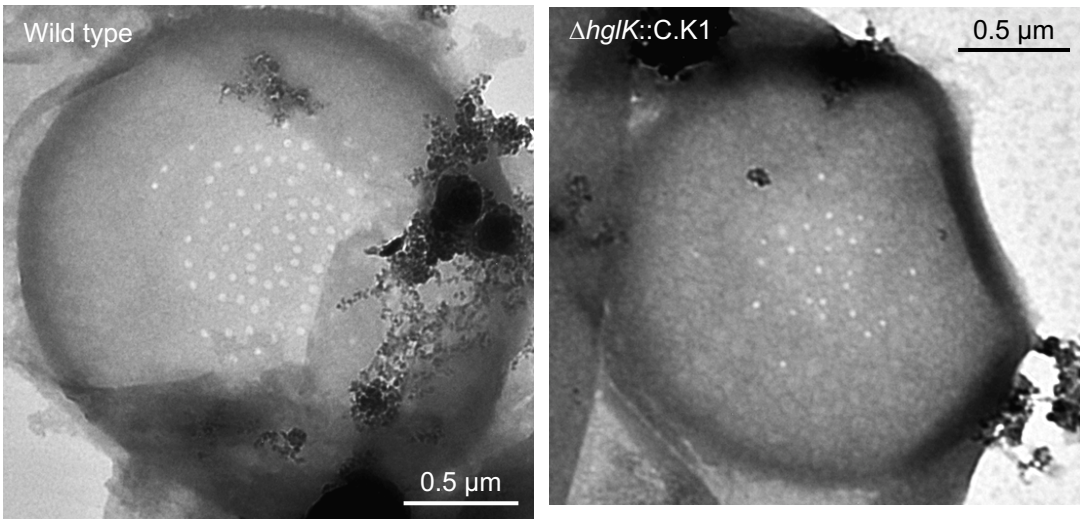

Strain	Nanopore number		Nanopore diameter (nm)	
	Mean ± SD (n)	*p*	Mean ± SD (n)	*p*
***Anabaena* (WT)**	39 ± 21 (26)		14.3 ± 9.3 (140)	
CSSA1 (Δ*hglK*::C.K1)	20 ± 13 (14)	0.003	15.8 ± 2.8 (179)	0.048

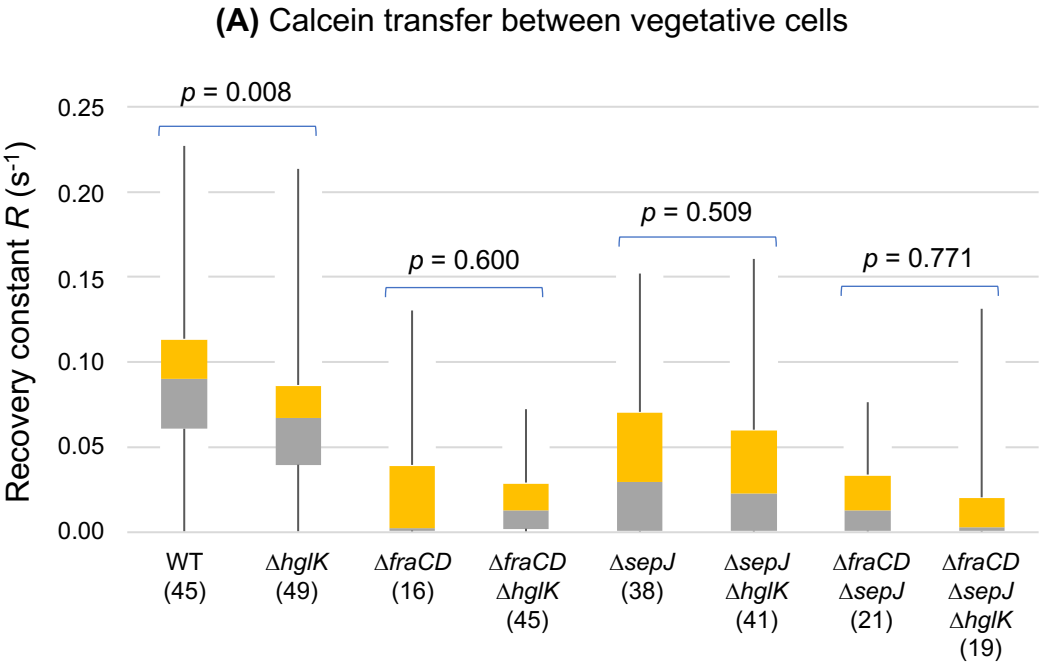
(A) Calcein transfer between vegetative cells
Recovery constant R (s^{-1})
0.25
0.20
0.15
0.10
0.05
0.00
p = 0.008
p = 0.600
p = 0.509
p = 0.771
WT (45)
Δ*hglK* (49)
Δ*fraCD* (16)
Δ*fraCD* Δ*hglK* (45)
Δ*sepJ* (38)
Δ*sepJ* Δ*hglK* (41)
Δ*fraCD* Δ*sepJ* (21)
Δ*fraCD* Δ*sepJ* Δ*hglK* (19)

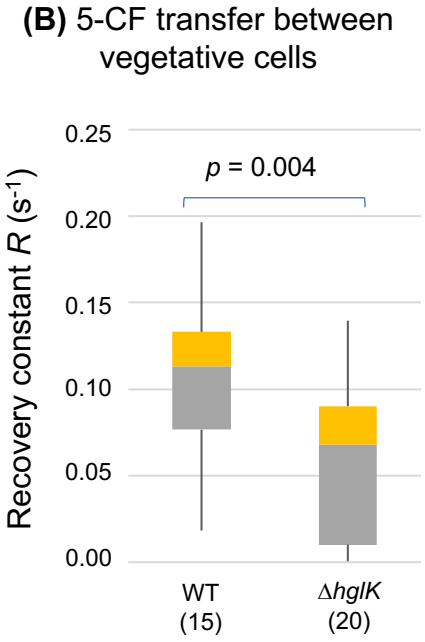
(B) 5-CF transfer between vegetative cells
Recovery constant R (s^{-1})
0.25
0.20
0.15
0.10
0.05
0.00
p = 0.004
WT (15)
Δ*hglK* (20)

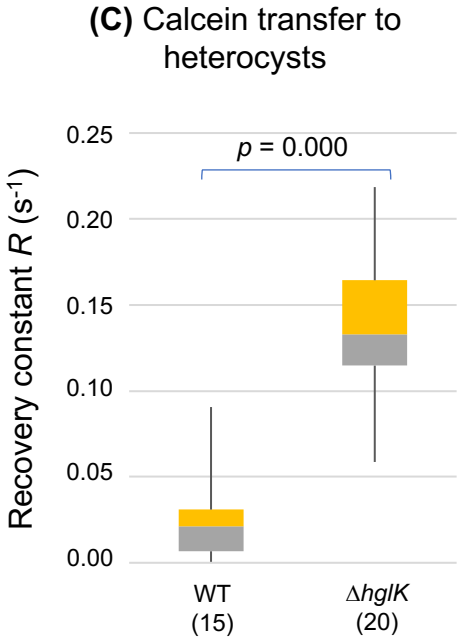
(C) Calcein transfer to heterocysts
Recovery constant R (s^{-1})
0.25
0.20
0.15
0.10
0.05
0.00
p = 0.000
WT (15)
Δ*hglK* (20)

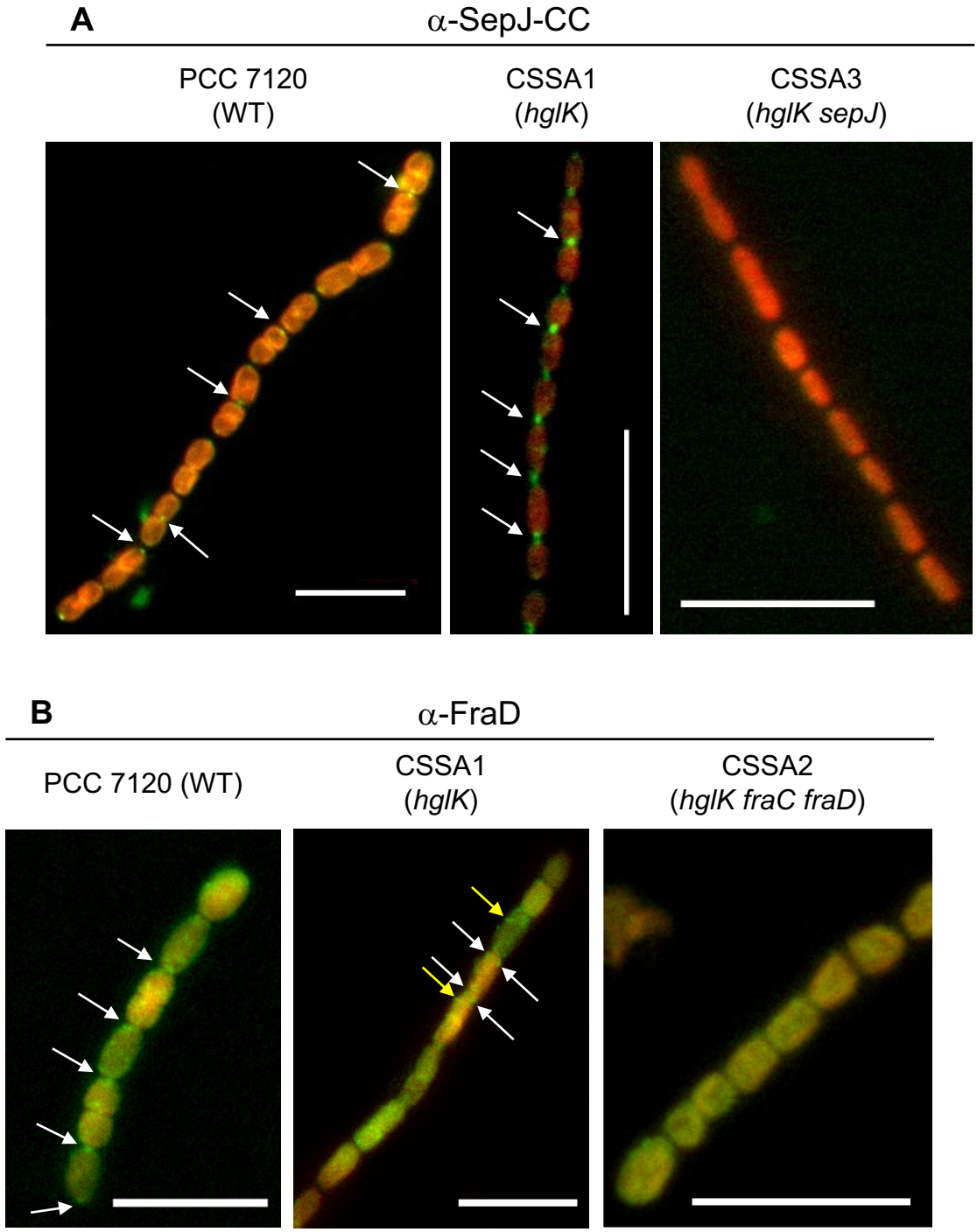
A
α-SepJ-CC
PCC 7120
(WT)
CSSA1
(hglK)
CSSA3
(hglK sepJ)
B
α-FraD
PCC 7120 (WT)
CSSA1
(hglK)
CSSA2
(hglK fraC fraD)